J|A|C|S ARTICLES

Published on Web 07/02/2009

Revealing a Second Transmetalation Step in the Negishi Coupling and Its Competition with Reductive Elimination: Improvement in the Interpretation of the Mechanism of Biaryl Syntheses

Qiang Liu,[†] Yu Lan,[‡,§] Jing Liu,[†] Gang Li,[†] Yun-Dong Wu,[*,‡,§] and Aiwen Lei[*,†,⊥]

College of Chemistry and Molecular Sciences, Wuhan University, Wuhan, Hubei 430072, China, College of Chemistry, Peking University, Beijing, China, Department of Chemistry, The Hong Kong University of Science and Technology, Clear Water Bay, Kowloon, Hong Kong, China, and State Key Laboratory of Organometallic Chemistry, Shanghai Institute of Organic Chemistry, Chinese Academy of Science, 354 Fenglin Lu Shanghai, 200032, China

Received March 26, 2009; E-mail: aiwenlei@whu.edu.cn; chydwu@ust.hk

Abstract: This paper presents an experimental and theoretical investigation of the Pd-catalyzed Negishi coupling reaction and reveals a novel second transmetalation reaction between an $Ar^1-Pd-Ar^2$ species and the organozinc reagent Ar^2-ZnX. Understanding of this second step reveals how homocoupling and dehalogenation products are formed. Thus, the second transmetalation generates Ar^2PdAr^2 and Ar^1ZnCl, which upon reductive elimination and hydrolysis, respectively, give the homocoupling product Ar^2-Ar^2 and the dehalogenation product Ar^1H. The ratio of the cross-coupling product Ar^1-Ar^2 and the homocoupling product Ar^2-Ar^2 is determined by competition between the second transmetalation and reductive elimination steps. This mechanism is further supported by density functional theoretical calculations. Calculations on a series of reactions suggest a strategy in controlling the selectivity of cross-coupling and homocoupling pathways, which we have experimentally verified.

Introduction

Transition-metal-catalyzed cross-coupling reactions have become extremely useful in organic syntheses.[1] Because of the recent emergence of a large number of drug candidates containing biaryls,[2] Pd- and Ni-catalyzed coupling of aryl halides and aryl metal species has been extensively studied.[1,3−6] Although transmetalation is an essential step in these catalytic reactions, the mechanism of this step is not well studied especially for Negishi coupling.[7] Understanding this essential step will enhance the development of this important class of reactions and increase their synthetic utility. For example, it is well known that the formation of homocoupling byproducts is a serious limitation to synthetic chemists and an obstacle to larger industrial-scale development.[8] We show in this paper that the selectivity of an important cross-coupling reaction, the Negishi coupling, is sometimes strongly affected by the transmetalation step.

Scheme 1. General Catalytic Cycle of Biaryl Syntheses

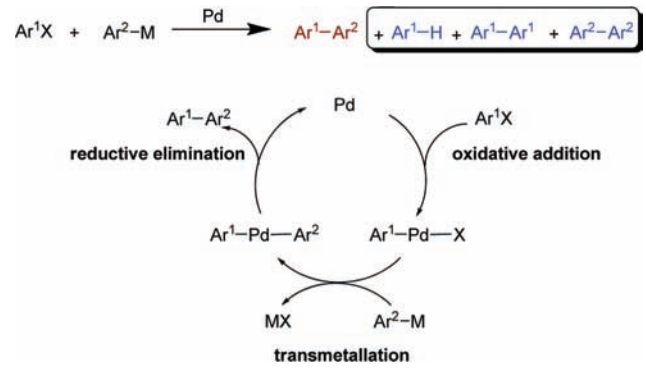

A well-accepted catalytic cycle of cross-coupling reactions is shown in Scheme 1, which includes three successive steps: oxidative addition of Ar^1X with the Pd catalyst, transmetalation with Ar^2M to furnish the key intermediate $Ar^1-Pd-Ar^2$, and reductive elimination to yield the desired cross-coupling biaryls and to regenerate the catalyst.[4] However, the cross-coupling reaction sometimes affords not only the cross-coupling product but also the products of dehalogenation, Ar^1-H, and homocoupling, Ar^1-Ar^1 and Ar^2-Ar^2,[1,9−19] for which there are

[†] Wuhan University.
[‡] Peking University.
[§] The Hong Kong University of Science and Technology.
[⊥] Shanghai Institute of Organic Chemistry, Chinese Academy of Science.

(1) Anastasia, L.; Negishi, E.-i. In *Handbook of Organopalladium Chemistry for Organic Synthesis*; 2002; Vol. 1, pp 311−334.
(2) Corbet, J.-P.; Mignani, G. *Chem. Rev.* **2006**, *106*, 2651–2710.
(3) Hassan, J.; Sevignon, M.; Gozzi, C.; Schulz, E.; Lemaire, M. *Chem. Rev.* **2002**, *102*, 1359–1469.
(4) Meijere, A. d.; Diederich, F. *Metal-Catalyzed Cross-Coupling Reactions*, 2nd ed.; Wiley-VCH: Weinheim, 2004.
(5) Negishi, E.-i. *J. Organomet. Chem.* **2002**, *653*, 34–40.
(6) Alberico, D.; Scott, M. E.; Lautens, M. *Chem. Rev.* **2007**, *107*, 174–238.
(7) Casares, J. A.; Espinet, P.; Fuentes, B.; Salas, G. *J. Am. Chem. Soc.* **2007**, *129*, 3508–3509.
(8) Banno, T.; Hayakawa, Y.; Umeno, M. *J. Organomet. Chem.* **2002**, *653*, 288–291.
(9) Alimardanov, A.; Schmieder-van de Vondervoort, L.; de Vries, A. H. M.; de Vries, J. G. *Adv. Synth. Catal.* **2004**, *346*, 1812–1817.

almost no well-accepted mechanisms. Understanding these mechanisms will help to optimize the catalytic cross-coupling toward the desired reaction pathway.

While oxidative addition and reductive elimination of Pd-catalyzed coupling reactions have been extensively studied both experimentally and theoretically,[7,20−46] the transmetalation reaction involving $Ar^1-Pd-Ar^2$ has only been sparsely studied.[47,48] In this paper, we report an experimental and theoretical study of the Pd-catalyzed Negishi coupling reaction of Ar^1I with Ar^2ZnCl. This study provides insight into the transmetalation of Negishi coupling and leads to the development of a strategy that maximizes the selectivity toward cross-coupling products. Here we report these results and this new strategy.

Table 1. Negishi Coupling of ArI with PhZnCl[a]

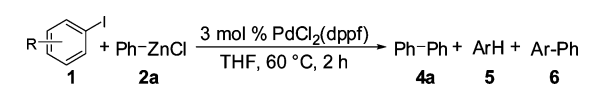

1 2a 4a 5 6

entry	R		yield %[b] 4a	5	6
1	2-CO_2Et	**1a**	76	70	18
2	4-CO_2Et	**1c**	trace	0	99[c]
3	2-$CONMe_2$	**1d**	39	38	61
4	2-CONHBu	**1e**	50	60	40
5	2-MeO	**1f**	29	19	65[c]
6	4-MeO	**1g**	13[c,d]	0	86[c]
7	2-^{i} Pr	**1h**	14	20	79
8	4-^{i} Pr	**1i**	trace	trace	99
9	2,4,6-trimethyl	**1j**	22	17	77

[a] The reactions were conducted with 0.5 mmol of **1**, 1 mmol of **2a**, and 3 mol % of $PdCl_2$(dppf) in THF at 60 °C for 2 h. [b] The yield was determined by GC. [c] Isolated yield. [d] 4,4′-Dimethoxybiphenyl (**7**) was detected.

Results and Discussion

1. Observation of Formation of Dehalogenation and Homocoupling Side Products. During the course of studying the Negishi coupling reaction using diene ligand **3**,[49] we examined the reaction of ethyl *o*-iodobenzoate (**1a**) with phenylzinc chloride (**2a**) as shown in eq 1. Although this is usually regarded as a "standard" Negishi coupling for biaryl syntheses, surprisingly, we found only trace amounts of the cross-coupling biaryl product **6a** was formed, and, instead, the major products were biphenyl **4a** and deiodoarylation product **5a**. Furthermore, we noticed that **4a** and **5a** were formed in almost equal amounts. We screened 10 additional Pd catalysts and ligands (see Table S1 in the Supporting Information) and generally found that this reaction produced considerable levels of homocoupling and dehalogenation products.

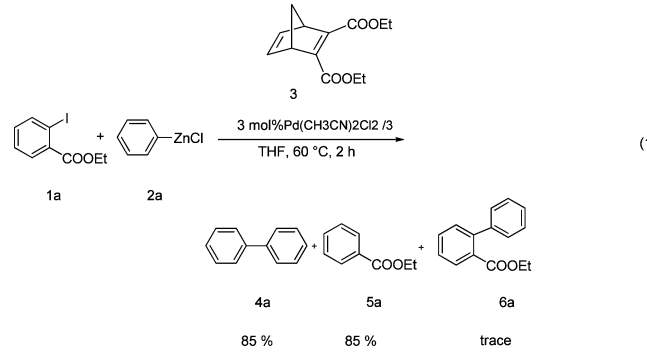

To further clarify this trend, reactions exploring different aryl iodide electrophiles with phenylzinc chloride **2a** using $PdCl_2$(dppf) as the catalyst were examined, and the results were presented in Table 1. Compared with ethyl *o*-iodobenzoate **1a**,

(10) Bumagin, N. A.; Ponomarev, A. B.; Beletskaya, I. P. *Zh. Org. Khim.* **1987**, *23*, 1354–1364.
(11) Bumagin, N. A.; Ponomarev, A. B.; Beletskaya, I. P. *Zh. Org. Khim.* **1987**, *23*, 1345–1353.
(12) Organ, M. G.; Ghasemi, H.; Valente, C. *Tetrahedron* **2004**, *60*, 9453–9461.
(13) Okamoto, Y.; Yoshioka, K.; Yamana, T.; Mori, H. *J. Organomet. Chem.* **1989**, *369*, 285–290.
(14) Negishi, E.; Takahashi, T.; Akiyoshi, K. *J. Organomet. Chem.* **1987**, *334*, 181–194.
(15) Bumagin, N. A.; Ponomarev, A. B.; Beletskaya, I. P. *J. Organomet. Chem.* **1985**, *291*, 129–132.
(16) Tsai, F.-Y.; Lin, B.-N.; Chen, M.-J.; Mou, C.-Y.; Liu, S.-T. *Tetrahedron* **2007**, *63*, 4304–4309.
(17) Lau, K. C. Y.; Chiu, P. *Tetrahedron Lett.* **2007**, *48*, 1813–1816.
(18) Coelho, A. V.; de Souza, A. L. F.; de Lima, P. G.; Wardell, J. L.; Antunes, O. A. C. *Tetrahedron Lett.* **2007**, *48*, 7671–7674.
(19) Arcadi, A.; Cerichelli, G.; Chiarini, M.; Correa, M.; Zorzan, D. *Eur. J. Org. Chem.* **2003**, 4080–4086.
(20) Nova, A.; Ujaque, G.; Maseras, F.; Lledos, A.; Espinet, P. *J. Am. Chem. Soc.* **2006**, *128*, 14571–14578.
(21) Nilsson, P.; Puxty, G.; Wendt, O. F. *Organometallics* **2006**, *25*, 1285–1292.
(22) Ariafard, A.; Lin, Z.; Fairlamb, I. J. S. *Organometallics* **2006**, *25*, 5788–5794.
(23) Espinet, P.; Echavarren, A. M. *Angew. Chem., Int. Ed.* **2004**, *43*, 4704–4734.
(24) Crociani, B.; Antonaroli, S.; Beghetto, V.; Matteoli, U.; Scrivanti, A. *Dalton Trans.* **2003**, 2194–2202.
(25) Ricci, A.; Angelucci, F.; Bassetti, M.; Lo Sterzo, C. *J. Am. Chem. Soc.* **2002**, *124*, 1060–1071.
(26) Casares, J. A.; Espinet, P.; Salas, G. *Chem.−Eur. J.* **2002**, *8*, 4843–4853.
(27) Franz, A. K.; Woerpel, K. A. *J. Am. Chem. Soc.* **1999**, *121*, 949–957.
(28) Casado, A. L.; Casares, J. A.; Espinet, P. *Organometallics* **1997**, *16*, 5730–5736.
(29) Louie, J.; Hartwig, J. F. *J. Am. Chem. Soc.* **1995**, *117*, 11598–11599.
(30) Perez-Temprano, M. H.; Nova, A.; Casares, J. A.; Espinet, P. *J. Am. Chem. Soc.* **2008**, *130*, 10518–10520.
(31) Hills, I. D.; Netherton, M. R.; Fu, G. C. *Angew. Chem., Int. Ed.* **2003**, *42*, 5749–5752.
(32) Goossen, L. J.; Koley, D.; Hermann, H.; Thiel, W. *Chem. Commun.* **2004**, 2141–2143.
(33) Ananikov, V. P.; Musaev, D. G.; Morokuma, K. *Eur. J. Inorg. Chem.* **2007**, 5390–5399.
(34) Surawatanawong, P.; Fan, Y.; Hall, M. B. *J. Organomet. Chem.* **2008**, *693*, 1552–1563.
(35) Braga, A. A. C.; Morgon, N. H.; Ujaque, G.; Maseras, F. *J. Am. Chem. Soc.* **2005**, *127*, 9298–9307.
(36) Henriksen, S. T.; Norrby, P.-O.; Kaukoranta, P.; Andersson, P. G. *J. Am. Chem. Soc.* **2008**, *130*, 10414–10421.
(37) Kozuch, S.; Shaik, S. *J. Am. Chem. Soc.* **2006**, *128*, 3355–3365.
(38) Yan, X.-X.; Peng, Q.; Li, Q.; Zhang, K.; Yao, J.; Hou, X.-L.; Wu, Y.-D. *J. Am. Chem. Soc.* **2008**, *130*, 14362–14363.
(39) Ahlquist, M.; Fristrup, P.; Tanner, D.; Norrby, P.-O. *Organometallics* **2006**, *25*, 2066–2073.
(40) Ahlquist, M.; Norrby, P.-O. *Organometallics* **2007**, *26*, 550–553.
(41) Ananikov, V. P.; Musaev, D. G.; Morokuma, K. *Organometallics* **2005**, *24*, 715–723.
(42) Braga, A. A. C.; Ujaque, G.; Maseras, F. *Organometallics* **2006**, *25*, 3647–3658.
(43) Goossen, L. J.; Koley, D.; Hermann, H. L.; Thiel, W. *Organometallics* **2005**, *24*, 2398–2410.
(44) Li, Z.; Fu, Y.; Guo, Q.-X.; Liu, L. *Organometallics* **2008**, *27*, 4043–4049.
(45) Lucassen, A. C. B.; Shimon, L. J. W.; Van der Boom, M. E. *Organometallics* **2006**, *25*, 3308–3310.
(46) Senn, H. M.; Ziegler, T. *Organometallics* **2004**, *23*, 2980–2988.
(47) Ozawa, F.; Fujimori, M.; Yamamoto, T.; Yamamoto, A. *Organometallics* **1986**, *5*, 2144–2149.
(48) Cardenas, D. J.; Martin-Matute, B.; Echavarren, A. M. *J. Am. Chem. Soc.* **2006**, *128*, 5033–5040.
(49) Liu, Q.; Duan, H.; Luo, X.; Tang, Y.; Li, G.; Huang, R.; Lei, A. *Adv. Synth. Catal.* **2008**, *350*, 1349–1354.

Scheme 2. Possible Pathways for the Homocoupling and Dehalogenation Side Products

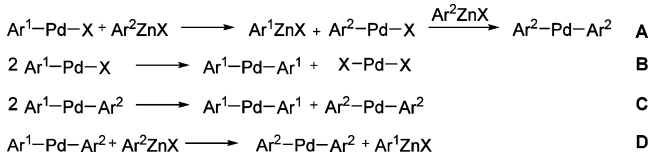

which gives only a small amount of cross-coupling product, the reaction of ethyl *p*-iodobenzoate (**1c**) with phenylzinc chloride **2a** yielded exclusively the cross-coupling product (Table 1, entry 2). However, other *ortho*-substituted aryl iodides containing electron-withdrawing or electronic-rich groups showed similar reactivity with phenylzinc chloride **2a** as with ethyl *o*-iodobenzoate **1a** and generated significant amounts of homocoupling biphenyl and reduction products (Table 1, entries 3−5, 7, and 9). The reactions of *para*-substituted aryl iodides with phenylzinc chloride **2a** exhibited excellent selectivity favoring the cross-coupling products (Table 1, entries 2, 6, and 8).

Four possible pathways for the formation of homocoupling and dehalogenation side products are shown in Scheme 2. Pathway A involves a transmetalation of the oxidative addition intermediate Ar^1-Pd-X with Ar^2ZnX to form Ar^2-Pd-X. This species undergoes a second transmetalation to give $Ar^2-Pd-Ar^2$ that results in the formation of homocoupling product Ar^2-Ar^2. This pathway was proposed by Elsevier et al. for the coupling reaction of benzyl bromide and *p*-TolM (M = MgBr or ZnBr) in the presence of Pd catalyst using Ar−BIAN (dimethyl fumarate) as the supporting ligand.[50] Pathway B involves disproportionation of Ar^1-Pd-X, which leads to the formation of $Ar^1-Pd-Ar^1$ and PdX_2. Pathway C involves disproportionation of $Ar^1-Pd-Ar^2$, which leads to the formation of $Ar^1-Pd-Ar^1$ and $Ar^2-Pd-Ar^2$ and gives homocoupling side products Ar^1-Ar^1 and Ar^2-Ar^2. Although the disproportionation has been observed in stoichiometric reactions,[28,51−58] pathways B and C cannot explain the formation of dehalogenation side product Ar^1-H. Since we observe that homocoupling and dehalogenation products are formed in equal amounts, this suggests that the pathways leading to these two products are related. Recently, Casares and Espinet et al. observed the transmetalation between $PdRfMe(PPh_3)_2$ (Rf = 3,5-dichloro-2,4,6-trifluorophenyl) and Me_2Zn.[7] Thus, we propose pathway D. This pathway involves a second transmetalation between Ar^2ZnX and $Ar^1-Pd-Ar^2$, which leads to the formation of homocoupling and dehalogenation products.

To differentiate among these four pathways, stoichiometric experiments were carried out as shown in Scheme 3. When the oxidative addition intermediate **8** was reacted with only 1 equiv of phenylzinc chloride (**2a**), the reaction generated the cross-coupling product **6b** in 95% yield. Further addition of **2a** to the reaction mixture led to no reaction. However, when the same reaction was carried out in the presence of 5 equiv of **2a**, the products **4a**, **5b**, and **6b** were formed in 60%, 60%, and 40% yields, respectively. This product distribution is consistent with the proposed pathway D shown in Scheme 2. In this pathway, the initial transmetalation reaction results in the formation of $Ar^1-Pd-Ar^2$. Without excess Ar^2ZnCl, its reductive elimination yields the cross-coupling product. However, in the presence of excess Ar^2ZnCl, a second transmetalation reaction, which competes with reductive elimination, occurs, leading to the homocoupling product.

Scheme 4. Deuteration Experiment

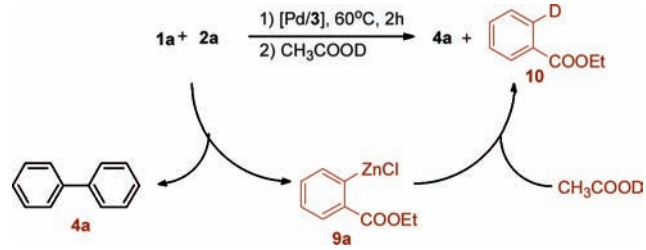

2. Identification of the Formation of Ar^1ZnI from the Reaction of Ar^1I with Ar^2ZnCl. For more information about the reaction mechanism, we carried out experiments to identify reaction intermediates and determine reaction kinetics. If pathway D in Scheme 2 operates, Ar^1ZnCl will be generated and subsequent hydrolysis will form the dehalogenated side product, Ar^1H. Therefore, to verify the hypotheses, it became a key issue to identify the formation of Ar^1ZnCl (Scheme 2, pathway D).

The first experiment involved deuteration (Scheme 4). The reaction of ethyl *o*-iodobenzoate **1a** with phenylzinc chloride **2a** was carried out at 60 °C for 2 h and then treated by CH_3COOD. As a result, the deuterated product **10** was observed. The molar ratio of **4a** to **10** is 1:1. This provides indirect evidence for the existence of Ar^1ZnCl in the reaction solution (Scheme 4).

The second attempt to identify 2-COOEtPhZnCl **9a** involved a trapping experiment shown in Scheme 5. In this experiment, ethyl *o*-iodobenzoate **1a** reacted with phenylzinc chloride **2a** at 60 °C for 2 h, and to the resulting mixture was added *p*-iodoanisole (**1g**). After an additional 2 h, the biaryl product **11** was isolated from this one-pot reaction in 56% yield. This supports the formation of arylzinc chloride **9a**, which then reacted with **1g** in the presence of palladium catalyst to afford **11**. This experiment provides additional evidence for the existence of 2-COOEtPhZnCl **9a** from the reaction of ethyl *o*-iodobenzoate **1a** with phenylzinc chloride **2a**.

To obtain evidence for the formation of the Ar^1ZnCl species that results from the second transmetalation, we also performed

Scheme 3. Stoichiometric Experiments

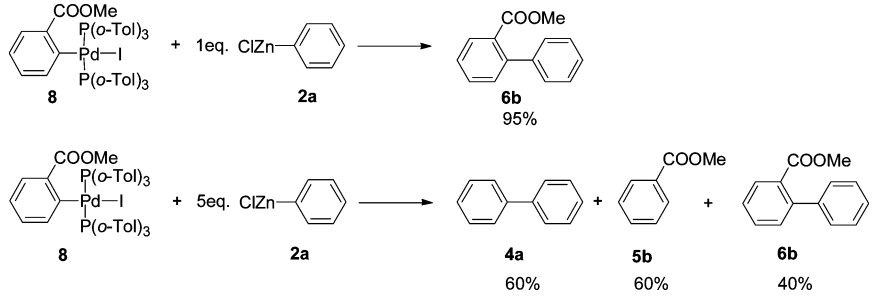

Scheme 5. Trapping Experiment

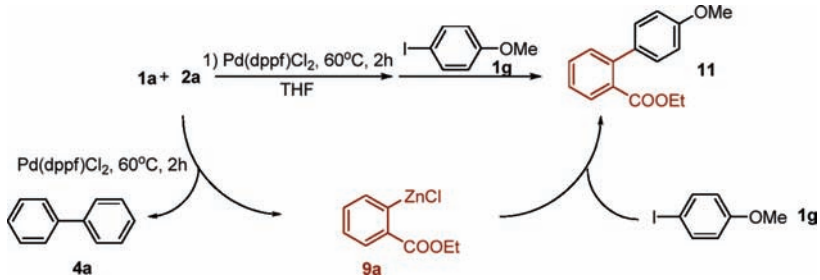

^{13}C NMR studies. First, we prepared an authentic sample of (*o*-MeOOCPh)ZnI from the reaction of methyl *o*-iodobenzoate **1b** with activated Zn dust in DMSO. The ^{13}C NMR of the carbonyl region shows a resonance at 166.2 ppm (Figure 1 B). In addition, the carbonyl region of **5b** shows a resonace at 167.0 ppm (Figure 1D) and **6b** shows a resonance at 169.1 ppm (Figure 1C). Second, the reaction of methyl *o*-iodobenzoate **1b** with phenylzinc chloride **2a** was performed in an NMR tube for 2 h, and the ^{13}C NMR of the reaction mixture was recorded. The spectrum (Figure 1A) shows two resonances. The resonance at 169.1 ppm is due to the product **6b**, as it matches the spectrum in Figure 1C. The resonance at 165.9 ppm nicely matches the resonance of (*o*-MeOOCPh)ZnI (166.2 ppm, Figure 1B) and confirms the identity of Ar^1ZnCl.

We also monitored the reaction of methyl *o*-iodobenzoate **1b** with phenylzinc chloride **2a** using *in situ* IR. The data are presented in Figure S1 and Figure S2 of the Supporting Information. Compared with an authentic sample, 2-MeOOC-PhZnCl **9b** is assigned as a newly formed component from the reaction of methyl *o*-iodobenzoate **1b** and phenylzinc chloride **2a**. Furthermore, kinetic profiles of starting materials of methyl *o*-iodobenzoate **1b** and the 2-COOMePhZnCl **9b** are listed in Figure 2. By plotting the linear region the observed reaction rate for the decline of **1b** was 1.33×10^{-3} $M \cdot s^{-1}$ (Figure 2C), and the observed rate for the increase of **9b** was 1.08×10^{-3} $M \cdot s^{-1}$ (Figure 2D). These kinetic data support the formation of **9b** from the reaction of **1b** with phenylzinc chloride **2a**.

3. Proposed Mechanism. The above experiments show the following: (1) The products of Ar^2-Ar^2 and Ar^1-H are formed in some of the reactions between Ar^1-I and Ar^2ZnCl, and they are derived from reductive elimination of Ar^2PdAr^2 and hydrolysis of Ar^1ZnCl, respectively. Both are derived from a second transmetalation between Ar^1PdAr^2 and Ar^2ZnCl. (2) The two products are formed in about the same amount. (3) The transmetalation between Ar^1PdI and Ar^2ZnCl gives Ar^2PdAr^1. These observations allow us to exclude the pathways shown in Scheme 2, eqs A−C, and to propose a mechanism for this Negishi reaction as shown in Scheme 6 using **1b** as an example. After the oxidative addition of **1b** to form **I**, first transmetalation results in the formation of intermediate **II**. While reductive elimination of **II** leads to the formation of the cross-coupling product **6b**, a second transmetalation can competitively occur to result in the formation of **9b** and intermediate **III**. Intermediate **III** undergoes rapid reductive elimination to give the homocoupling product **4a**, and the dehalogenation product comes from the hydrolysis of **9b**.

4. Theoretical Study. 4.1. The First Transmetalation Reaction. To support our proposed mechanism and to provide more insight into the nature of Negishi coupling, density functional calculations were performed. We first studied the transmetalation between **I** (in Scheme 6) and phenylzinc chloride. Our calculations used $Pd(Me_2P\text{-}CH_2\text{-}CH_2\text{-}PMe_2)$ as a model for the catalyst and coupling substrates methyl *o*-iodobenzoate **1b** and phenylzinc chloride **2a**. Complex **12** (Figure 3) was

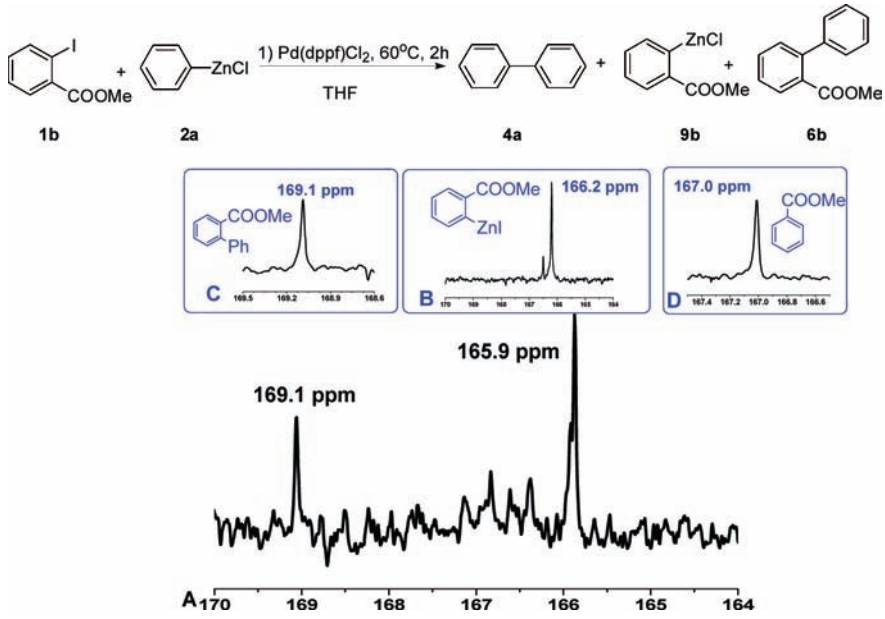

Figure 1. (A) ^{13}C spectrum of the reaction mixture starting from 0.5 mmol of **1b** and 1 mmol of **2a** in THF; (B) ^{13}C spectrum of authentic arylzinc reagent **9b** in DMSO; (C) ^{13}C spectrum of **6b** in $CDCl_3$; (D) ^{13}C spectrum of **5a** in $CDCl_3$.

Scheme 6. Proposed Mechanism

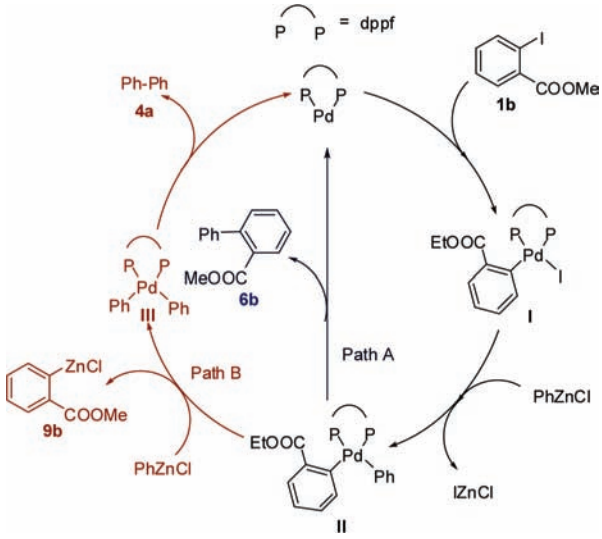

the starting structure. Because the complexation energy between phenylzinc chloride and the Ar−Pd complex could not be calculated accurately, the energy of this species was set to zero.

Our calculations suggest that there are two possible pathways for the transformation of **12**. The first pathway involves the replacement of the iodo ligand by the Ph group and results in the formation of **14**. The second pathway involves replacement of the aryl group on the Pd in **12** by the Ph on Zn group to give **16**.

The calculated activation free energy of the first pathway occurring through transition state **13-ts** is 18.6 kcal/mol, and the relative free energy of the transmetalation product **14** is 5.6 kcal/mol. Although the generation of **14** is calculated to be endergonic, aggregation of Zn(I)Cl is expected, which should result in a significant stabilization to make the reaction irreversible. In contrast, the calculated activation free energy for the second pathway occurring via transition state **15-ts** is 26.7 kcal/mol. Thus, in terms of free energy of activation, the first pathway is much more favorable than the second pathway by 8.1 kcal/mol. Since the first pathway gives an Ar^1PdAr^2 species, this result is in agreement with the experimental observations (Scheme 3) and supports the mechanism in Scheme 6.

4.2. Competition between Reductive Elimination of II (Scheme 6) and Second Transmetalation. After confirming the formation of intermediate **II** as shown in Scheme 6 as the product of the first transmetalation reaction, we turned our

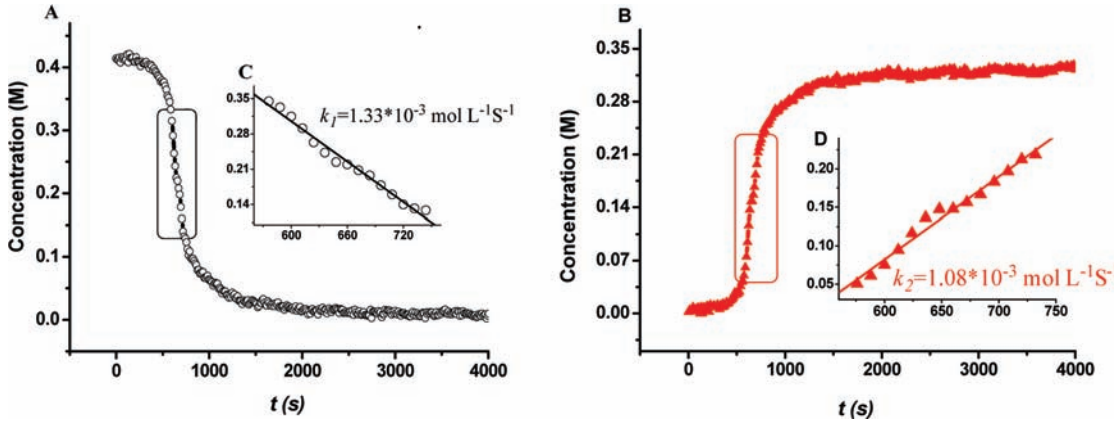

Figure 2. (A) Kinetic profile of [**1b**] vs *t*. (B) Kinetic profile of [**9b**] *vs t*. (C) Linear fit of part of the kinetic region of [**1b**] vs *t*. (D) Linear fit of part of the kinetic region of [**9b**] vs *t*.

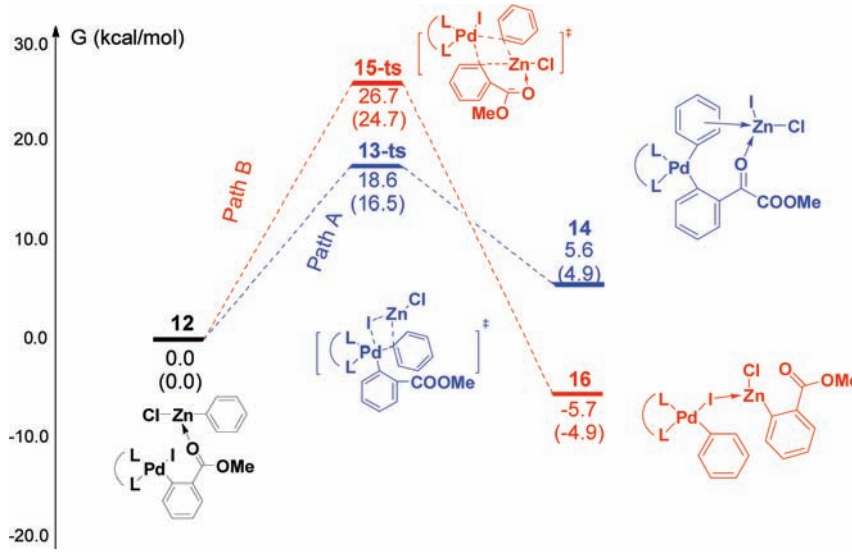

Figure 3. Free energy contrast of the two competitive transmetalation pathways.

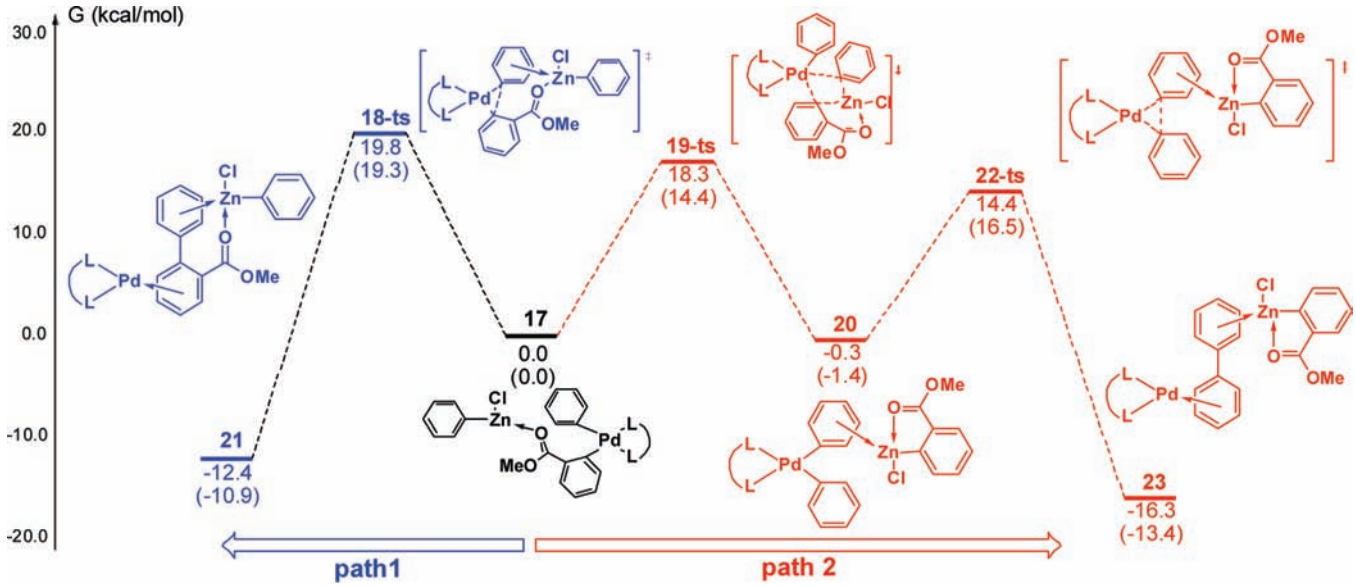

Figure 4. Free energy profile of the competition between reductive elimination (path 1) and transmetalation (path 2). The values are the calculated relative Gibbs free energies with solvation of THF. The values in parentheses are the calculated relative enthalpies in THF.

attention to the competitive reaction between reductive elimination and the second transmetalation with **II**. Again, the coordination energy of phenylzinc chloride and **II** could not be calculated exactly. Therefore, we set the **II**-PhZnCl complex **17** as the reference of the free energy surface. This approach makes the comparison of activation energy of reductive elimination and second transmetalation steps more reasonable because both are now unimolecular reactions, *vide infra*.

The calculated potential free energy surface of the reductive elimination and the second transmetalation reactions is shown in Figure 4. The calculated free energy of activation of the reductive elimination occurring through **18-ts** to form the cross-coupling biaryl product is 19.8 kcal/mol in THF solvent. We also calculated the same reaction without the coordination of phenylzinc chloride (Table 2) as 20.4 kcal/mol, indicating that the coordination of phenylzinc chloride has little effect on the reductive elimination. The reductive elimination reaction is calculated to be exergonic by 12.4 kcal/mol (see **21** in Figure 4).

The second transmetalation occurs through transition state **19-ts**. It has a calculated activation free energy of 18.3 kcal/mol, which is 1.5 kcal/mol lower than that of the reductive elimination reaction. In fact, the second transmetalation product **20** is calculated to be slightly more stable than **17**. It undergoes reductive elimination through transition state **22-ts** with an activation free energy of 14.7 kcal/mol. This result is in qualitative agreement with the experimental observation that products **4a** (homocoupling) and **5a** (dehalogenation) are dominant when Ar^1I is **1a** (Table 1).

4.3. Controlling Factors for the Competition between Reductive Elimination and Second Transmetalation. To help design reactions that can effectively avoid homocoupling and dehalogenation reaction, it is important to understand how substitution patterns can influence the competition between reductive elimination and second transmetalation. For this purpose, a series of reactions were calculated. The calculated free energies of activation for the reductive elimination ($\Delta G_1^{\ddagger}$) and second transmetalation reaction ($\Delta G_2^{\ddagger}$) along with additional selected geometrical parameters are given in Table 2. The calculation results can be summarized as follows:

(1) For the parent system (entry 1), where both Ar^1 and Ar^2 are phenyl groups, the calculated $\Delta G_1^{\ddagger}$ and $\Delta G_2^{\ddagger}$ are 16.7 and 22.3 kcal/mol, respectively. The results show that without a substituent on the two aryl groups the second transmetalation hardly occurs due to the 5.6 kcal/mol activation energy difference. This is in agreement with experiment.

(2) When Ar^1 bears a *para*-substituent (entries 2, 3), $\Delta G_1^{\ddagger}$ is slightly increased. The most significant effect is the electron-withdrawing ester group on $\Delta G_2^{\ddagger}$, which is increased by about 3 kcal/mol. Thus, a *para* electron-withdrawing substituent on Ar^1 favors the reductive elimination with respect to the second transmetalation, while a *para* electron-donating group has the opposite effect, although both effects are mild.

(3) When Ar^1 has an *ortho* substituent (entries 4−6), the barrier to reductive elimination is increased by 2−4 kcal/mol. The barrier to the second transmetalation is reduced by the ester group (by 2.7 kcal/mol) and methoxyl group (by 0.7 kcal/mol), probably due to the Zn−O coordination in the transition state. This is increased by about 1 kcal/mol by an isopropyl group. In the case of entry 7, where Ar^1 has two *ortho* methyl groups, the steric effect is increased, resulting in a further increase in both $\Delta G_1^{\ddagger}$ and $\Delta G_2^{\ddagger}$. Overall, the steric effect by the *ortho* substituent(s) in Ar^1 is more significant in the reductive elimination transition state than in the transmetalation transition state.

(4) The last four entries in Table 3 indicate that when the Ar^2 has an *ortho* substituent, the free energy of activation of the second transmetalation reaction ($\Delta G_2^{\ddagger}$) is significantly increased. The transition state apparently is very sensitive to the steric effect of the *ortho* substituent in Ar^2.

To understand the above results, we analyzed the steric effect in transition states. Shown in Figure 5 are selected calculated structures with some geometrical parameters. For example, $L_2PdAr^1Ar^2$ **26** takes on a nearly square-planar geometry. The Ar^1 and Ar^2 are both perpendicular to the L_2Pd plane, so that they have no repulsion with each other. In the reductive elimination transition state, **27**, the C1---C2 distance is shortened

Table 2. Calculated Activation Free Energies of Reductive Elimination ($\Delta G_1^{\ddagger}$) and Second Transmetalation ($\Delta G_2^{\ddagger}$) and Selected Geometric Information of **24-ts** with Different Substitutuens (free energies in kcal/mol, bond lengths in Å)

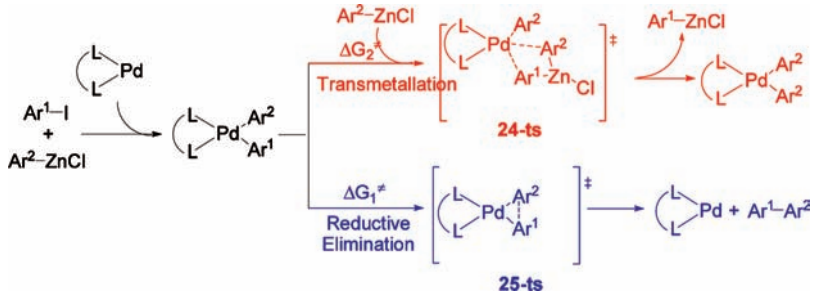

Entry	R^1	R^2	ΔG_1	ΔG_2	$\Delta G_2(\text{Corr})^{a}$	Geometry information of **24-ts**					
						$L_{Zn\text{-}C2}$	$L_{Zn\text{-}C3}$	$L_{Pd\text{-}C2}$	$L_{Pd\text{-}C3}$	$D_{P1\text{-}P2\text{-}Pd\text{-}C2}$	$D_{P1\text{-}P2\text{-}Pd\text{-}C3}$
1	H	H	16.7	22.3	19.5	2.02	2.02	3.06	2.95	-148.0°	135.2°
2	MeOOC	H	17.2	25.4	22.6	2.02	2.01	3.05	3.02	-148.5°	135.1°
3	MeO	H	18.0	22.5	19.7	2.01	2.02	3.09	2.90	-149.2°	133.4°
4	H	COOMe	20.4	21.6	18.8	2.11	2.04	2.82	2.91	-146.3°	128.9°
5	H	OMe	18.7	21.6	18.8	2.03	2.03	2.96	2.87	-145.5°	134.9°
6	H	H	20.6	23.4	20.6	2.02	2.03	3.06	2.94	-146.9°	135.3°
7	H	H	22.8	24.7	21.9	2.03	2.03	3.05	3.13	-133.6°	153.2°
8	H	COOMe	20.4	31.4	28.6	2.01	2.10	3.28	2.68	-153.0°	125.3°
9	H	OMe	18.7	27.3	24.5	2.02	2.03	3.11	2.93	-147.4°	135.0°
10	H	H	20.6	30.3	27.5	2.00	2.03	3.76	3.06	-169.3°	124.2°
11	H	H	22.8	35.3	32.5	2.02	2.02	3.40	3.25	-159.8°	132.4°

[a] $\Delta G_2(\text{Corr})^{\ddagger} = \Delta G_2^{\ddagger} - 2.8$ kcal/mol, based on free volume theory for bimolecular reactions in solution.[44]

to about 1.95 Å, while both Pd−C1 and Pd−C2 distances are only slightly lengthened compared to the distance in **26**. In **27**, both phenyl groups maintain a perpendicular conformation and the shortest H/H distance between the two phenyl groups is 2.2 Å, indicating that when an *ortho* substituent is introduced, a significant steric interaction will occur.

Structure **30** is the transition state of the second transmetalation for the parent system (entry 1 of Table 3). While the spectrator phenyl group still coordinates with Pd in the L_2Pd plane with a perpendicular conformation, the two phenyl groups that are involved in transmetalation are pointing up and down the L_2Pd plane, respectively. They are nearly coplanar with each other but have to adopt a conformation so that they coordinate Pd through their π faces. The Pd−C2 and Pd−C3 distances are close to about 3.0 Å, significantly longer than a normal Pd−C bond. On the other hand, the two Zn−C bonds are 2.02 Å. Thus, the transition state can be considered as a zwitterionic species with the Pd moiety positively charged and the Zn moiety negatively charged.

There is a short distance of 2.60 Å between the two designated *ortho* hydrogens in **30b**. This indicates that when one is replaced by a bulky substituent, steric interaction will be introduced. Structures **31** and **32** are the transition states for the second transmetalation of entries 4 and 6, respectively.

Table 3. Biaryl Syntheses through Negishi Coupling without Homocoupling Products[a]

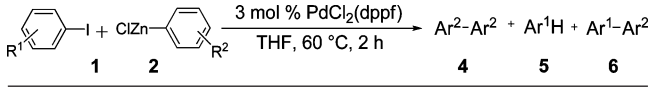

1 2 4 5 6

entry	R^1		R^2		yield[b] % 4	5	6
1	H	(**1k**)	2-CO_2Et	(**9a**)	trace	nd	94
2	4-MeO	(**1i**)	2-CO_2Et	(**9a**)	trace	0	97
3	4-CO_2Et	(**1c**)	2-CO_2Et	(**9a**)	trace	nd	92
4	H	(**1k**)	2-^{i}Pr	(**2b**)	trace	nd	99
5	4-MeO	(**1i**)	2-^{i}Pr	(**2b**)	trace	0	90
6	4-CO_2Et	(**1c**)	2-^{i}Pr	(**2b**)	trace	trace	88
7	H	(**1k**)	2,4,6-trimethyl	(**2c**)	trace	nd	90
8	4-CO_2Et	(**1c**)	2,4,6-trimethyl	(**2c**)	trace	0	75
9	H	(**1k**)	2-MeO	(**2d**)	3[c]	nd	95
10	4-MeO	(**1i**)	2-MeO	(**2d**)	6[c]	nd	93

[a] The reactions were conducted with 0.5 mmol of ArI, 1 mmol of ArZnCl, and 3 mol % of $PdCl_2$(dppf) in THF at 60 °C for 2 h. "nd" means "not determined". [b] Isolated yield. [c] GC yield.

In both structures, the phenyl group with the substituent (COOMe in **31** and *i*-Pr in **32**) rotates by about 24−32° so that the above-mentioned steric interaction is avoided. This rotation of phenyl group only slightly affects the bonding in Pd−C2 and Zn−C2. Thus, the steric interaction of the substituent can be largely avoided. This explains the results shown in entries 4−7 of Table 3, where an *ortho* substituent in Ar^1 only slightly increases the free energy of activation of the second transmetalation ($\Delta G_2^{\ddagger}$). In fact, in the cases of COOMe and OMe substituents, $\Delta G_2^{\ddagger}$ is even reduced compared to the parent system due to electrostatic interactions of these substituents with Zn.

The situation for Ar^2 with an *ortho* substituent is very different. The spectrator aryl group in the second transmetalation is Ar^2. Inspection of structure **30** reveals that the spectrator phenyl group orients in such a way that its two *ortho* hydrogens point to the other two phenyl groups, resulting in two short C---H distances of 3.06 and 2.82 Å, respectively. When either of them is replaced by a bulky group, significant steric interactions will be introduced. This is indeed the case. Structure **33** is the transition state of transmetalation for entry 10. Due to the isopropyl group in the spectrator aryl (Ar^2), the top aryl group (Ar^1) suffers such large interactions that it has to move away from the Pd. The Pd−C3 distance changes from 3.0 Å in other structures to 3.7 Å in **33**.

To make the comparison between $\Delta G_1^{\ddagger}$ and $\Delta G_2^{\ddagger}$ more meaningful, some adjustment to $\Delta G_2^{\ddagger}$ is necessary. The reductive elimination is a unimolecular reaction; thus, the calculated entropy contribution to free energy of activation is reasonable. However, since the second transmetalation reaction is a bimolecular reaction, and it is difficult to accurately estimate the activation entropy for this reaction because it is a solution-based reaction, we corrected the activation free energy $\Delta G_2^{\ddagger}$ based on the free volume theory.[44] This provides a rate of a solution-based bimolecular reaction that is about 80 times faster than the corresponding reaction in the gas phase. This means that the activation free energy for solution reaction should be about 2.8 kcal/mol smaller than the value calculated in the gas phase. The adjusted activation free energies $\Delta G_2^{\ddagger}$ are given as $\Delta G_2(\mathrm{Corr})^{\ddagger}$.

Our calculation results can easily explain the experimental observations shown in Table 1. When Ar^1 is *para* substituted (entries 2 and 8 in Table 1), only the cross-coupling product is observed, and the calculation results in Table 2 indicate that the reductive elimination has a much lower barrier ($\Delta G_1^{\ddagger}$) than the second transmetalation ($\Delta G_2^{\ddagger}$). However, when Ar^1 has an *ortho* substituent (entries 1, 3−5, 7, and 9 in Table 1), a mixture of cross-coupling and homocoupling products is experimentally observed. An explanation for this comes from the theoretical calculations; as for the *ortho*-substituents (entries 4−7 in Table 2), the free energies of activation of reductive elimination and second transmetalation steps are comparable.

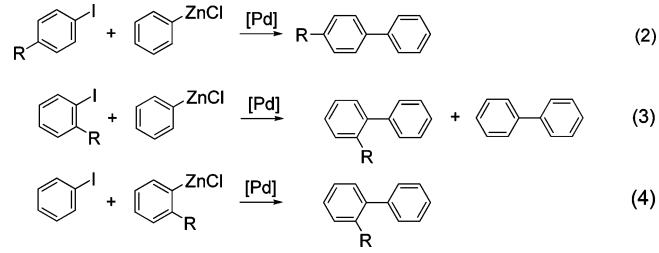

The results in entries 8−11 of Table 2 are most interesting. They suggest that if Ar^2ZnCl bears an *ortho* substituent, although the substituent increases the barrier of reductive elimination, it has a greater effect on the barrier of second transmetalation such that it effectively blocks the formation of homocoupling and dehalogenation products (eq 4). Thus, through theoretical insight, we can propose an experimental strategy for a more efficient synthesis of *ortho*-substituted biaryl compounds using the Negishi coupling reaction, which is to *use a less substituted* Ar^1-I *and a more substituted* Ar^2ZnCl.

5. Experimental Verification. We have conducted a series of experiments to test the above strategy (eq 4) for the formation of biaryl compounds. These results are summarized in Table 3. *Cross-coupling products are produced in high yields for all the tested reactions*. Since the above theoretical calculations suggested a strategy of matching less-substituted Ar^1-I and more subsituted Ar^2-ZnCl, we are gratified to provide experimental evidence that indeed this strategy works toward exclusively generating the cross-coupled biaryls.

Conclusion

In summary, the $Ar^1-Pd-Ar^2$ is traditionally considered as the key intermediate leading to the reductive elimination step that provides the cross-coupling products in the Negishi coupling reaction. In this paper, we report the observation of a second transmetalation step that occurs between the key intermediate $Ar^1-Pd-Ar^2$ and the organozinc reagent Ar^2-ZnX. This critical insight provides the first understanding of how dehalogenated and homocoupling products are formed in the Negishi reaction. Indeed, an initial transmetalation step gives the Ar^1PdAr^2 species; however, we show that a second transmetalation step between Ar^2ZnX with Ar^1PdAr^2 provides Ar^2PdAr^1 and Ar^1ZnX. These species lead to the homocoupling and dehalogenated products, respectively. DFT calculations show that a critical competition occurs in the second transmetalation and reductive elimination steps. These calculations indicate that an *ortho* substituent in Ar^1I favors the second transmetalation reaction, while an *ortho* substituent in Ar^2ZnCl significantly disfavors a second transmetalation. This suggests a strategy to avoid homocoupling and dehalogenation side product formation, i.e., to

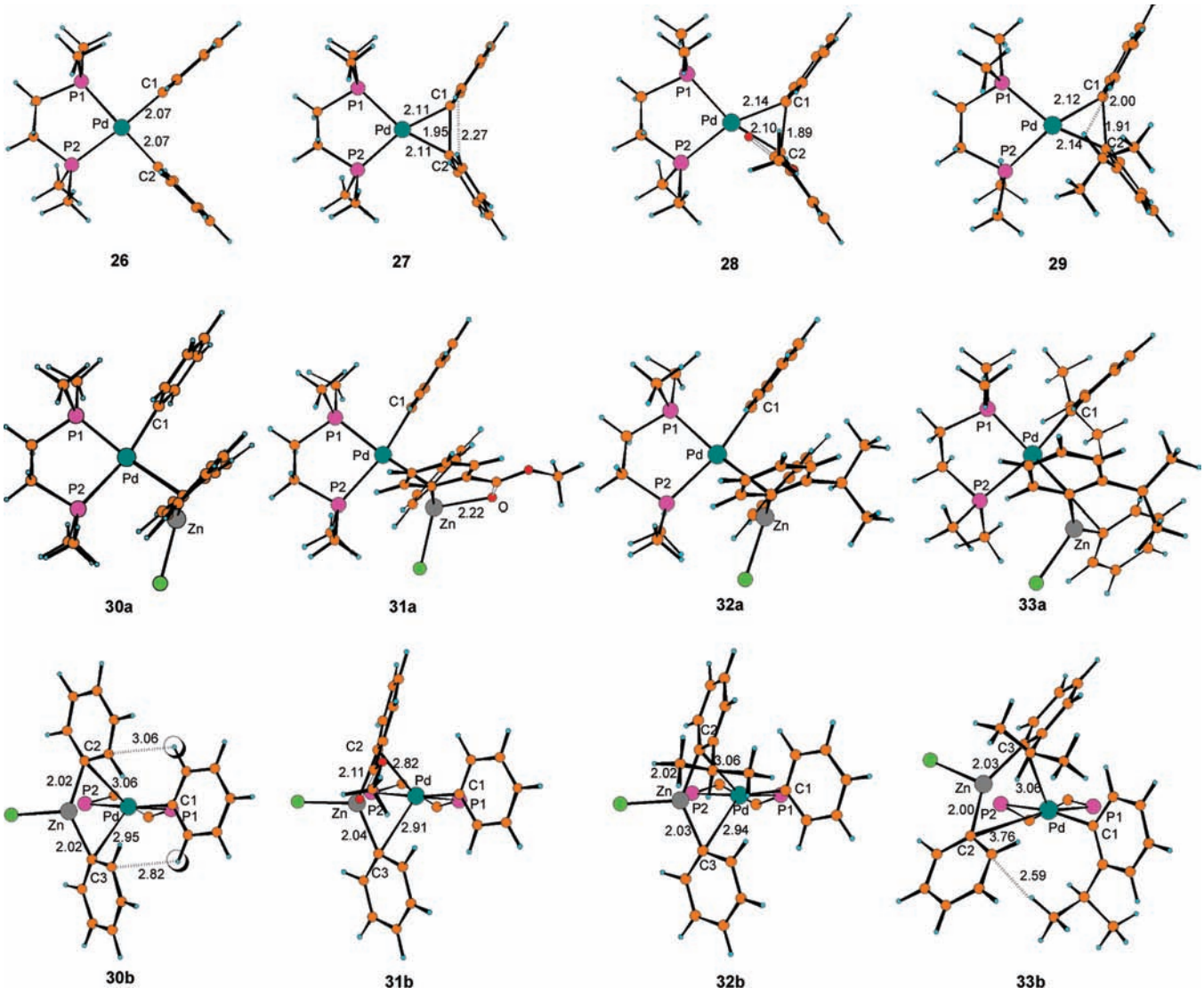

Figure 5. Calculated geometries of selected intermediates and transition states in Table 3: **26** and **27** are intermediate and reductive transition states of entry 1; **28** and **29** are reductive transition states of entries 4 and 6, respectively; **30**, **31**, **32**, and **33** are transition states of transmetalation of entries 1, 4, 6, and 10, respectively.

choose a less sterically crowded Ar^1I and use an *ortho*-substituted Ar^2ZnCl. This strategy has been experimentally proven to work for the simplest case (Table 3). Overall, this paper provides considerable experimental and theoretical insight into the mechanism of transmetalation for Negishi coupling.

Experimental Section

General Procedure for Negishi Coupling. Under nitrogen, $PdCl_2$(dppf) (0.015 mmol) and an iodoaryl (0.5 mmol) were dissolved in THF (0.5 mL). Then, to this THF solution was added the aryl zinc reagent (1 mmol). The mixture, which immediately turned black, was stirred for 2 h at 60 °C. The reaction was quenched with saturated aqueous ammonium chloride solution, separated, and then extracted with ethyl acetate. The organic layer was dried over sodium sulfate, filtered, and concentrated. Purification of products was accomplished by silica gel chromatography.

Computation Methodology. All calculations were carried out with the GAUSSIAN 03 package.[59] The Becke proposed hybrid

(50) van Asselt, R.; Elsevier, C. J. *Organometallics* **1994**, *13*, 1972–1980.
(51) Ozawa, F.; Kurihara, K.; Fujimori, M.; Hidaka, T.; Toyoshima, T.; Yamamoto, A. *Organometallics* **1989**, *8*, 180–188.
(52) Giovannini, R.; Stuedemann, T.; Devasagayaraj, A.; Dussin, G.; Knochel, P. *J. Org. Chem.* **1999**, *64*, 3544–3553.
(53) Kraatz, H.-B.; Van der Boom, M. E.; Ben-David, Y.; Milstein, D. *Isr. J. Chem.* **2001**, *41*, 163–171.
(54) Casado, A. L.; Espinet, P. *Organometallics* **1998**, *17*, 3677–3683.
(55) Tsou, T. T.; Kochi, J. K. *J. Am. Chem. Soc.* **1979**, *101*, 7547–7560.
(56) Yagyu, T.; Hamada, M.; Osakada, K.; Yamamoto, T. *Organometallics* **2001**, *20*, 1087–1101.
(57) Suzaki, Y.; Osakada, K. *Organometallics* **2003**, *22*, 2193–2195.
(58) Ozawa, F.; Hidaka, T.; Yamamoto, T.; Yamamoto, A. *J. Organomet. Chem.* **1987**, *330*, 253–263.
(59) Frisch, M. J.; et al. *Gaussian 03*, revision C.02; Gaussian, Inc.: Wallingford, CT, 2004.
(60) Becke, A. D. *J. Chem. Phys.* **1993**, *98*, 5648–5652.
(61) Lee, C.; Yang, W.; Parr, R. G. *Phys. Rev. B: Condens. Matter* **1988**, *37*, 785–789.
(62) Cances, E.; Mennucci, B.; Tomasi, J. *J. Chem. Phys.* **1997**, *107*, 3032–3041.
(63) Cances, E.; Mennucci, B.; Tomasi, J. *J. Chem. Phys.* **1998**, *109*, 260–266.
(64) Cossi, M.; Barone, V.; Mennucci, B.; Tomasi, J. *Chem. Phys. Lett.* **1998**, *286*, 253–260.
(65) McQuarrie, D. A. *Statistical Mechanics*; Harper and Row: New York, 1976.

(B3),[60] together with the Lee−Yang−Parr (LYP)[61] correlation functionals, has been chosen for this work. The SDD basis set was used for Pd, Zn, and I atoms. The standard all-electron 6-31G(d) basis set was used for all the other atoms. Aqueous phase single-point energies were carried out at the same level using the self-consistent reaction field method (SCRF), by the integral equation formalism polarizable continuum model[62−64] (IEFPCM) with THF solvent. Frequencies, thermal corrections, and entropies were calculated at this level of theory using the standard statistical mechanical method at 298 K.[65]

Acknowledgment. We thank Dr. Shen Hong of Merck & Co., Inc. and Professor John Sowa of Seton Hall University for their kind help in revising the manuscript. This work was supported by National Natural Science Foundation of China (20832003, 20772093, 20502020, and 20225312), the Excellent Youth Foundation of Hubei Scientific Committee, and specialized Research Fund for the Doctoral Program of Higher Education (20060486005), and the Research Grants Council of Hong Kong (N_HKUST 623/04).

Supporting Information Available: Spectroscopic data, experiments details, and DFT calculation details are available free of charge via the Internet at http://pubs.acs.org.

JA903277D